Ultra-thin supported lipid monolayer with unprecedented mechanical and dielectric properties

Ahmad Kenaan, Racha El Zein, Volkan Kilinc, Sébastien Lamant, Jean-Manuel Raimundo, Anne Charrier

DOI: 10.1002/adfm.201801024

Advanced functional Materials

Article type: Full paper

Ultra-thin supported lipid monolayer with unprecedented mechanical and dielectric properties

Ahmad Kenaan, Racha El Zein, Volkan Kilinc, Sébastien Lamant, Jean-Manuel Raimundo, Anne M. Charrier**

Dr. A. Kenaan, Dr. R. ElZein, V. Kilinc, Dr. S. Lamant, Prof. J.-M. Raimundo, Dr. A.M. Charrier
Aix Marseille Univ, CNRS, CINAM, Marseille, France

E-mail: charrier@cinam.univ-mrs.fr; jean-manuel.raimundo@univ-amu.fr

Keywords: Supported lipid monolayer, ultra-thin dielectric, mechanical properties, dielectric properties, lipid engineering

ABSTRACT

The development of ultra-thin dielectrics for low power electronics operations, flexible and printed electronics, and field effect transistors based sensors is still a challenge. Here monolayers of engineered lipids supported on silicon are reported presenting exceptional mechanical and dielectric properties. The lipid monolayers are stabilized using a simple procedure based on a two-stage reticulation process in both their aliphatic chains and their head-group. With a

thickness lower than 3 nm, such layers are demonstrated to offer exceptional mechanical and dielectric stability with unprecedented low leakage current and dielectric strength. Surprisingly, the mechanical and dielectric pressures required to rupture/breakdown the monolayers are shown to be similar. These results suggest the presence of a strong correlation between mechanical and dielectric properties, as well as between the mechanisms of rupture and breakdown.

1. Introduction

With the development of flexible and printed electronics, organic dielectrics have been investigated extensively in the past decade.[1,2] They are chiefly used in organic (OFETs) and thin film (TFT) transistors as gate dielectric materials with performances combining low leakage current, high breakdown strength, large capacitance, good mechanical flexibility and stability which in some cases near or surpass those of amorphous (*a*-Si) or poly crystalline (*c*-Si) silicon.[3,4] Moreover for low power operations in TFT it is meaningful to maintain the dielectric thickness as thin as possible.[5] To this aim, nano-dielectrics such as nanoparticles or self-assembled monolayers or multilayers have been recently developed and implemented in OFETs.[6–9] Another class of material, the supported lipid layers, with thicknesses of a few nanometers also constitutes good candidates. In living cells lipid membrane forms indeed a natural insulator[10] which plays an efficient role as barrier to both ionic and electronic transport associated with an electrical resistance of the order of several giga-Ohms in magnitude.[11,12] These unique properties make them very attractive to be used as ultra-thin dielectric layer in electronic devices and have recently raised interest, marked by the increasing number of studies reporting the formation of lipid layers on various substrates such as silicate,[13] H-terminated silicon surface,[14,15] gold,[16] alkylated surfaces[17] and more recently graphene,[18-20] graphene-oxide[20] or polymeric substrates such as PEDOT:PSS.[21] So far in most studies lipid layers have

been used as biocompatible interfaces or as ionic barriers in field effect transistors to study ion channels in lipid membranes.[22-25] However, despite excellent insulating properties, lipid bilayers and even more lipid monolayers have been poorly exploited in devices due to their inherent instability under application of an electric field, leading to damages caused mainly by an electroporation process occurring at low electric field (1 MV/cm).[26-30] Furthermore a lack of mechanical stability is often observed. Layers are stabilized on substrates by van der Waals interactions whereas the layer integrity is maintained by hydrophobic forces between the lipids aliphatic chains. Drying off or exposing the sample to solvents usually induces lipid layer destruction, therefore limiting its use to applications in solution as well as its storage. Several strategies have been carried out in order to overcome these issues including the direct substrate surface bonding[31,32] or the internal crosslinking within the plane of the lipid layer.[20,33] Interestingly, it was previously shown that the mechanical force required to disrupt a self-assembled monolayer made from 1,2-bis-(10,12-tricosadiynoyl)-*sn*-glycero-3-phosphocholine (DC8,9PC or DC-PC) (SLM, Supported Lipid Monolayer) can be aptly improved, by a factor of ten, after a radical reticulation within the plane of the monolayer.[19] This property has been successfully exploited in the fabrication of a field effect transistor sensors based on modified SLMs, as ultra-thin gate dielectric layers, directly immobilized at the surface of a H-terminated silicon-based channel.[34,35] Additional experiments performed on SLM's arrays fabricated using harsh lift-off processes, and used as capacitive sensing platform clearly confirmed these improvements.[36] In these studies, SLMs were subjected to electric fields up to 6 MV/cm, i.e. to values much higher than those at which electroporation occurs. Surprisingly these results seem to indicate that the mechanical stability was accompanied with a substantial increase of the dielectric stability suggesting that the cross-linking approach may constitute a beneficial strategy to achieve powerful ultrathin dielectric and must be pursued.

In the present work we aim at studying the relationship between mechanical and dielectric stabilities of SLMs and at investigating new routes to further strengthen them. Dense SLMs on Si-H surfaces are readily obtained according to a synthetic procedure developed in our group from the vesicle fusion method.[18,19] Subsequently an innovative two-step process is used to mechanically stabilize the dielectric monolayer. This process encompasses two consecutive crosslinking reactions respectively at the inner and outer side of the monolayer. At each step, mechanical and electrical stabilities were carefully investigated. Thereby, mechanical stability is ascertained by quantifying the force necessary to rupture the monolayer from indentation measurements using an atomic force microscope (AFM) and the dielectric properties is determined by measuring both the leakage current, the dielectric strength and the lifetime at a constant electric field.

2. Results and discussion

2.1 Making of the lipid monolayers

Several different SLMs were obtained from pristine DC-PC, a commercially available lipid, and from modified ones (**Table 1**). DC-PC lipids have been chosen due to their intrinsic structural properties that can be useful for subsequent changes both at the inner and outer parts of the supported monolayers. The phosphocholine head group of the DC-PC derivative can be easily cleaved with a phospholipase[34] affording a free hydroxyl group (DC-Glycerol) that can be further converted to other functions or appropriately modified. For instance, in the course of this study DC-MTS and DC-OTS layers were achieved by reacting the free OH group with methyltrichlorosilane (MTS) or Trichloro(octadecyl)silane (OTS) respectively. The genesis and properties of these novel dielectric layers will be discussed below. In addition, DC-PC lipids possess in their aliphatic chain acetylenic groups that can be used to reticulate the lipids in the

plane of the layer in order to ensure a greater molecular cohesion and therefore stability. This crosslinking, named herein reticulation **1**, consists of a radical reticulation reaction initiated by AAPH (2,2'-Azobis(2-methylpropionamidine) as a heat-sensitive water-soluble free radical initiator. At this stage the supported lipid monolayer exhibits sufficient stability to be rinsed with solvent or dried and can be further easily manipulated.[36] Using this procedure, DC-Glycerol-R monolayers were obtained and have been used as the starting point to generate the DC-MTS and DC-OTS layers as depicted in **Figure 1**. The supported DC-Glycerol monolayer was first cross-linked using the reticulation **1** process to give DC-Glycerol-R and then secondly the free OH groups were reacted with the alkyltrichlorosilane derivatives leading to a second reticulation (reticulation **2**) at the outer side of the SLM resulting in end-capping the dielectric layer. As reference, a non-reticulated supported DC-Glycerol monolayer was also made and tested. Homogeneity of the different lipid layers is shown on the AFM images (Fig. 1(A'-C')) with a surface roughness below 0.7 nm in all cases. Their thickness was determined by making a hole across the layer with an AFM tip and reported in Table 1. All results are in perfect agreement with what is expected according to the length of the deposited lipid.

2.2. Effect reticulation on the lipid monolayer mechanical properties

The effect of reticulation on the mechanical stability of the layers was investigated using DC-glycerol, DC-Glycerol-R, and DC-MTS layers. These layers have roughly the same thickness and differ mainly by the number of reticulations. As a probe of stability we measured the normal force that needs to be applied to the layer by an AFM tip to make the tip rupture the layer. For each layer, a minimum of 240 independent indentation measurements were performed on at least three samples. All experiments were done in water in order to minimize capillary forces. During indentation measurement, the layer may resist to the tip penetration until the force is large enough

to break-through the layer.[19,37] This rupture is evidenced on the force curves as a jump of the tip to the substrate surface at a given loading force (see **Figure 2**). Figure 2B summarizes the results and reports the average rupture forces that were extracted from the force measurements for each layer (the corresponding data points are shown in **Figure S1**). In the case of DC-Glycerol, a very small mechanical resistance is observed and the tip can easily penetrate throughout the layer. From 400 measurements, only 113 times rupture forces were measurable, the rest of the curves showing no resistance of the layer to the tip (the rupture force was smaller than the resolution of our experimental setup and hence could not be measured). Nevertheless, based on the measurable data, an average breakthrough force was found at a value of 0.25±0.17 nN, which therefore is over-estimated. After reticulation **1**, *i.e.* internal reticulation, the rupture force measured on DC-Glycerol-R is enhanced by a factor of 6 (1.59±0.65 nN), demonstrating a significant effect of the reticulation process on the monolayer resistance to normal forces. In the case of DC-MTS layer, the rupture force is further raised by a factor of 2.3 to a value of 3.74±1.06 nN with respect to DC-Glycerol-R. Furthermore, the thicknesses of the layers before and after each reticulation process remain unchanged, proving that the enhancement of the mechanical stability comes undoubtedly from the reticulation and not, for instance, from an increase of the layer thickness[38] (Here the layer thickness is determined for each point as the tip jump distances obtained experimentally from the force measurements, see Figure S1) .

It is generally accepted that the rupture of a layer is an activated process. An energy barrier has to be overcome which corresponds to the activation energy for the formation of a hole in the layer which is large enough to initiate tip penetration. [38] For DC-PC layers, it was shown in a previous work that this activation energy which increases with the indentation rate, by a factor of 3 after reticulation **1** (DC-PC-R) is related to the lipids diffusion coefficient in the layer.[18] Moreover, El Zein et al. estimated the reduction of diffusion coefficient from ~10^{-12} cm²/s to ~10^{-14} cm²/s after

reticulation **1** which was associated to the formation of nano-domains or chains of reticulated lipids.[39] With the additional reticulation **2**, the size of the nano-domains/chains is expected to increase hence reducing the diffusion coefficient of the lipids even more. This could explain the increase of the force needed to induce the layer rupture with the consecutive reticulations.

2.3. Dielectric properties of reticulated layers

In a different set of experiments we investigated the effect of reticulation on the lipid monolayers dielectric properties by measuring both, monolayers leakage current and lifetime when exposed to a constant electric field.

2.3.1 Densities of leakage current

The measurements were performed in air and we focused on the reticulated layers, *i.e.*, DC-Glycerol-R, DC-MTS and DC-OTS. Examples of JV curves (Current density (J) vs Voltage (V)) are shown in **Figure S2** for the three types of layers for V (Starting from 0V, the measurement was stopped after dielectric breakdown occurred, i.e. V_{max} varied between 2 and 15 V depending on the measurement). In contrast with DC-MTS and DC-OTS which J-V curves are very reproducible, for DC-Glycerol-R a high variability is observed from curve to curve and the signal is quiet noisy, hence revealing lesser stability. From the median curves (**Figure 3A**), at low voltage, all three layers show similar J with values lower than 10^{-7} A/cm². As the voltage is increased, J also increases linearly with V in different proportions with $J_{DC\text{-}Glycerol\text{-}R} > J_{DC\text{-}MTC} > J_{DC\text{-}OTS}$ reaching values of ~10^{-5} A/cm², ~5.10^{-7} A/cm² and ~5.10^{-8} A/cm² respectively at 2 V. This effect gets even more pronounced at higher voltage; at 4V, DC-Glycerol-R reaches a saturation current (limited by the apparatus) which corresponds to the dielectric breakdown of the layer. In contrast J remains low for both DC-MTS and DC-OTS with values of J of ~5.10^{-6} A/cm²

and ~1.10^{-7} A/cm² respectively. An important difference in median absolute deviation can be also noted with high values for DC-Glycerol-R and much lower values for DC-MTS and DC-OTS measurements, therefore reflecting the variability in DC-Glycerol-R measurements and the stability of DC-MTS and DC-OTS. This is emphasized in the average current densities (Figure S2D) with higher differences even at low voltage. DC-Glycerol-R and DC-MTS have similar length and only differentiate by the reticulation **2** at the head-group. The decrease in J of several orders of magnitude hence shows the effect of additional reticulation **2** on improving the insulating properties of the lipid monolayer. This improvement is even more enhanced with DC-OTS with an additional gain of 1 order of magnitude. The difference between DC-MTS and DC-OTS arises from the length of the aliphatic chains in the MTS and OTS groups from 1 to 18 carbons respectively. -$(C\text{-}C)_n$- chains are known to be good insulators[40,41] and are therefore responsible for the decrease of the leakage current. The results reported herein are rather unique; comparing with dielectrics of similar thickness as the densities of leakage current are at least 1 order of magnitude lower than those reported for oxide layers produced by rapid thermal processing (RTP) (10^{-6} A/cm² at 1V for a 2.2 nm thick oxide layer)[42] and 3 orders of magnitude lowers than for high-κ dielectrics (10^{-4} A/cm² at 0.5V for a 4 nm thick HfO_2 layer on graphene).[43]

The difference between DC-Glycerol and DC-MTS can be explained by considering the lipid molecules as flexible chains and the inter-molecular bonds due to reticulation as consolidating structures. In DC-Glycerol-R, the upper part (above the reticulation bonds) of the lipid layer can splay under the electric field,[31] hence creating opened and disorganized regions with reduced insulating performances. It was indeed shown that for self-assembled monolayers of long alkyl chains the leakage current density varies drastically with the chain length (for small chain length

it is mainly due to electron tunneling through the layer [44]) as well as with the compacity and ordering of the layer.[45] In DC-MTS, the upper part is stabilized by the reticulation **2** and prevents splaying, thus conserving an effective aliphatic chain of 20 carbons (~2 nm). For The high variability observed in DC-Glycerol-R J-V curves could therefore be explained by a disorganization of the upper part of the lipids under the electric field, hence confirming the drastic effect of the reticulation as a stabilizing process.

2.3.2 Lifetime of lipid monolayers under a constant electric field: Determination of dielectric strength

The second parameter we tested deals with the lifetime of the lipid layer under an electric field (E). This parameter is crucial for devices applications to estimate their life expectancy. To this aim constant voltage is applied to the layer and current is monitored until dielectric breakdown occurs. The latest shows as a sudden rise of the current leakage by several orders of magnitude (See **Figure S3**). To decipher the role of the reticulation on the dielectric strength and lifetime, measurements were performed on DC-Glycerol, DC-Glycerol-R, and DC-MTS layers that differ mostly by the number of reticulations. The results are reported in **Figure 3B**. In the following the direct breakdown electric field (E_{DB}) is defined as the dielectric strength at which the monolayer breaks within less than one minute at a given electric field value. For DC-glycerol, E_{DB} is very low, it occurs at typically 1-2 MV/cm, suggesting that such monolayer is hardly usable as a dielectric in a device. Such value coincides indeed with those that have been reported in the literature for the electroporation of lipid layers.[29,46,47] For DC-glycerol-R and DC-MTS monolayers the lifetime was measured for E in the range [10-23 MV/cm] and [27-55 MV/cm] respectively. For both these layers the lifetime decreases exponentially with increasing E as indicated by the corresponding curve fits (yellow and blue lines respectively). Such an exponential decay of the lifetime with the electric field was already reported for thin polymer

films.[48] Remarkably, both curves are strongly shifted towards high E and exhibit much higher values of E_{DB} reaching ~20 MV/cm and ~35 MV/cm for DC-Glycerol-R and DC-MTS respectively.

To evaluate the effect of the aliphatic chain length on dielectric breakdown, similar measurements were performed with DC-OTS layers. The lifetime displayed versus the electric field (**Figure S4 (a))** shows a similar curve as described before for DC-Glycerol-R and DC-MTS with an E_{DB} at ~20 MV/cm, i.e. much smaller than for DC-MTS. However, by plotting the lifetime versus the applied voltage both DC-MTS and DC-OTS are perfectly superimposed (**Figure S4 (b))**. Interestingly, these results show that the length of the aliphatic chain at the head-group in DC-OTS although playing a major role in reducing the leakage current, does not impact on the breakdown voltage. The latter is hence determined by the number of reticulations.

Remarkably, for all cases, the values of E_{DB} are much higher than those reported for silicon oxide,[49] with a layer of same thickness, which fall in the range of 10-15 MV/cm or high-κ dielectric layers which vary approximately as the reverse of the dielectric constant (For example E_{DB} of 5.7 MV/cm and 11.5 MV/cm were reported for a 59 nm HfO_2 layer and a 63 nm layer of Si_3N_4 respectively) .[50,51] In addition, the electrical energy per unit area for dielectric breakdown can be calculated for each surface using E_{DB} according to $\bar{T} = T + 1/2\, \varepsilon\varepsilon_0 {E_{DB}}^2 h$,[28,30] with T the average layer tension considered equal to zero, ε_0 the vacuum permittivity, and h the thickness of the lipid layer. The lipid layer dielectric constant of all lipid layers was assumed similar in the calculation, i.e. ε=2.4.[52,53] For the DC-Glycerol layer, a value of $\bar{T}$ of 0.9 dyne.cm^{-1} has been obtained coherently with previously reported data on supported lipid bilayer.[28,30] However for DC-Glycerol-R, DC-MTS and DC-OTS the values of $\bar{T}$ increased dramatically to 92 dyne.cm^{-1} and 286 dyne.cm^{-1} and 183 dyne.cm^{-1} respectively and outstrip by far the previous

reported results (*i.e.* in the range 0.4-30 dyne.cm^{-1}).[28,30] All these results demonstrate the impact of the double reticulation on the dielectric performances of the lipid layer.

2.4 Relationship between mechanical rupture force and dielectric strength

Comparing the direct breakdown electric fields and mechanical rupture forces at every stage of the reticulation process, we notice an interestingly similar increase by factors of ~10 and ~2 after the reticulation **1** and the reticulation **2** respectively. This observation is quiet striking and may suggest that the rupture mechanisms of the lipid layer may be similar for both mechanical and electrical processes.

Both mechanisms have been studied theoretically in water for non-reticulated supported lipid layers[28,54] or cell membranes.[26,27,31] In the framework of nano-indentation experiments, Butt and *al*[51] developed a two-state film rupture reaction theory based on the assumption that an AFM tip can rupture the lipid layer after the formation of a sufficiently large hole under the tip. It correlates the force required to create a hole to the line tension energetic cost and considers that every molecule has binding sites with energetically favorable positions. When an AFM tip is pressed on the layer, inducing a mechanical pressure, it becomes energetically favorable for the molecules to jump to an adjacent free binding site and form a hole under the tip.[38,55-57] The mechanism of electroporation, which is widely discussed in cell biology is not fully understood yet. Several dynamical simulations have been developed to study the phenomenon, and they agree on the fact that electroporation is induced initially by the insertion of water molecules in the lipid layer whose dipoles reorganize with respect to the electric field. [26,27,54,58] The main mechanism for pore formation is a large difference in the dielectric constants of water (ε~80) and lipid layer (ε~2.5). The lipid layer can be considered as a planar capacitor, which tends to

increase its capacitance in order to minimize electric energy. The electric field pushes water molecules into the membrane to substitute the lipids with low dielectric constant, by water with high dielectric constant, thus creating an effective lateral pressure applied to the pore edge.[31] The result of this mechanism leads to a compression of the lipid layer, i.e. to an electrostatic pressure, which leads to the opening of a hole, similarly to the case of mechano-poration. The two mechanisms of mechanical rupture and dielectric breakdown may hence be both initiated by a normal pressure which depends on the energy required to displace the lipids.

Although these models were developed in an aqueous medium for non-reticulated lipids, we believe they can still be applied to describe our data in air (our electrical measurements) considering that DC-Glycerol-R head-group is hydrophilic and with a maximum grafting of MTS or OTS every two lipids (i.e. every 4 aliphatic chains), the MTS/OTS layers are poorly dense. Consequently, a molecular layer of water may be present at the air/lipid interface playing the role of water molecules reservoir. Clearly here instead of displacing individual lipid, pore formation in reticulated layers requires the displacement of the nano-domains/chains of reticulated lipids. In this case, we can anticipate that the displacement energy cost must be higher and so the normal pressure required to inducing this displacement.

To investigate this assumption the corresponding mechanical and electrostatic pressures were both calculated for DC-Glycerol, DC-Glycerol-R and DC-MTS layers. The mechanical pressure at rupture, $P_m = F_m/S$, was calculated using the rupture force obtained from the AFM indentation measurements, with S the tip-surface contact area. The breakdown electrostatic pressure (P_e) is defined by the force per unit area created when an electric field is applied across the lipid monolayer. It is given by $P_e = F_e/S = 1/2\,\varepsilon\varepsilon_0 E^2$ with $\varepsilon = 2.4$ the dielectric constant of the lipids,[52,53] ε_0 the vacuum permittivity and E the direct breakdown electric field. The results of such calculations (**Figure 4**) show that for each type of surface, the mechanical and electrostatic

pressures have similar values comforting the assumption that the mechanisms responsible both for mechanical rupture and dielectric breakdown might be the same and both initiated by a normal pressure which depends on the energy required to displace lipids, i.e. on the size of the reticulated lipid domains.

3. Conclusions

In conclusion, we have developed a method based on a two-stage reticulation process which allows the formation of lipid monolayers supported on silicon with high mechanical stability. We have shown that this double reticulation leads to improving drastically the dielectric properties of the lipid monolayer with dielectric performances which exceed by far the properties of inorganic dielectrics for equivalent thickness. These results suggest that such lipid monolayers are good candidates to be considered in the development of devices as ultrathin dielectric. Also, using the mechanical rupture forces and the dielectric breakdown electric field, we have demonstrated strong correlation between the electrical and mechanical properties. Surprisingly, we show that the mechanical and electrostatic pressures required to rupture/breakdown the layer, i.e., to making pores, have similar values, therefore suggesting similar pore formation processes whatever the stress is exerted mechanically or electrically. These results question the mechanism involved in pores formation in such reticulated lipid monolayers and a deep understanding of the processes would require the development of theoretical models.

4. Experimental section

Lipids cleavage: DC-Glycerol lipids are obtained after cleaving the phosphocholine head-groups of DC-PC lipids (23:2 diyne PC, Avanti Polar Lipids, Alabama) using a phospholipase C (Sigma Aldrich). 0.1% lipids in water are mixed with 10 μg phospholipase C at 50°C during 16 hours. After cooling down the solution to room temperature,

the organic phase was extracted two times with chloroform, dried over Mg_2SO_4, filtrated and the solvent was removed under reduced pressure. The product was finally dried under vacuum for three hours.

Supported lipid monolayer formation and reticulations processes: Lipid monolayer supported on H-terminated silicon surface was made using a protocol developed in our laboratory and based on the vesicle fusion method. Small unilamellar lipid vesicles were first fabricated: 100 µl of 0.1% lipid stock solution in chloroform are first heated at 50°C until the chloroform is evaporated, then re-diluted in 100 µl of deionized water. The lipid solution is then sonicated 30 min and extruded across 100 nm pores polycarbonate membranes. Just before lipid deposition, H-terminated silicon surfaces were obtained after etching native silicon oxide layer by dipping the silicon sample 2 minutes in 2% HF. The lipid solution is then poured onto the silicon surface at room temperature and then cooled down to 10°C. The temperature is then slowly increased to 32°C at 1°C/min. At this stage DC-Glycerol monolayer is formed. DC-Glycerol-R is obtained from DC-Glycerol by making a reticulation (Reticulation 1) of the aliphatic chains using the acetylenic groups of the lipid chains (Figure 1). It is induced by addition of 1% free radical AAPH (2,2′-Azobis(2-methylpropionamidine) dihydrochloride, Sigma Aldrich) in water and increasing the temperature to 42°C. After 45 minutes the sample is cooled down and rinsed with deionized water. DC-MTS and DC-OTS are obtained from DC-Glycerol-R by exposing the sample to 1 mmol solution of MTS (Methyltrichlorosilane, Sigma Aldrich) or OTS (Octadecyltrichlorosilane, Sigma Aldrich) in 1,4 dioxane (Sigma Aldrich) for 15 minutes. The sample is then rinsed with methanol to remove residual dioxane from the surface. This silanization leads to a second reticulation (Reticulation 2) of the lipid head-groups.

Surface imaging and indentation measurements by AFM: All measurements were realized using NTEGRA atomic force microscope from NT-MDT Spectrum Instruments (Moscow, Russia). Sample surface imaging was performed in tapping mode in air using NSC 35 cantilevers (Nanoandmore, USA) with a of diameter 8 nm and spring constant of ~15 N/m. Indentations measurements were performed in water using NSC 38 cantilevers with a diameter of 8 nm as verified by scanning electron microscopy and a spring constant of ~0.09 N/m. For each experiment the cantilever force constant was evaluated using the thermal noise analysis method[59] after calibrating the tip deflection against a hard silicon surface. For each type of lipid layer the measurements were reproduced on three different samples. The loading and unloading rates were fixed at a rate of 18 µm/s.

Electrical measurements: Measurements were performed in air using a homemade setup. Electrical contacts across the lipid layer were taken on the silicon substrate on one side and using a mercury drop on the other side. The contact area between the mercury drop and the sample was determined for each contact by making a picture. Contact areas were typically $2.5x10^{-6}$ cm². HP 4140 pico-ammeter was used and I(V) measurements were realized at a rate ranging from 10 to 100 mV/s.

Supporting Information

Supporting Information is available from the Wiley Online Library or from the author.

Acknowledgements

This work was financially supported by the Agence Nationale de la Recherche, under project N°ANR-16-JTIC-0003-01 and by the Societé d'Aide au Transfert Technologique du Sud-Est (SATT-Sud Est) under contract N°147680.

Conflict of interest

The authors declare no conflict of interest.

References

[1] A. Facchetti, M.-H. Yoon, T. J. Marks, *Adv. Mater.* **2005**, *17*, 1705.

[2] M. D. Noh, J. F. Antaki, M. Ricci, J. Gardiner, D. Paden, J. Wu, E. Prem, H. Borovetz, B. E. Paden, *Artif. Organs* **2008**, *32*, 127.

[3] J. Mei, Y. Diao, A. L. Appleton, L. Fang, Z. Bao, *J. Am. Chem. Soc.* **2013**, *135*, 6724.

[4] R. P. Ortiz, H. Yan, A. Facchetti, T. J. Marks, *Materials (Basel).* **2010**, *3*, 1553.

[5] L. Sun, G. Qin, J.-H. Seo, G. K. Celler, W. Zhou, Z. Ma, *Small* **2010**, *6*, 2473.

[6] M. R. Beaulieu, J. K. Baral, N. R. Hendricks, Y. Tang, A. L. Briseño, J. J. Watkins, *ACS Appl. Mater. Interfaces* **2013**, *5*, 13096.

[7] V. Malytskyi, J.-J. Simon, L. Patrone, J.-M. Raimundo, *RSC Adv.* **2015**, 5, 26308.

[8] L. Huang, Z. Jia, I. Kymissis, S. O'Brien, *Adv. Funct. Mater.* **2010**, *20*, 554.

[9] S. A. DiBenedetto, A. Facchetti, M. A. Ratner, T. J. Marks, *Adv. Mater.* **2009**, *21*, 1407.

[10] J. C. Weaver, K. H. Schoenbach, *IEEE Trans. Dielectr. Electr. Insul.* **2003**, *10*, 715.

[11] R. J. O'Neill, L. Tung, *Biophys. J.* **1991**, *59*, 1028.

[12] C. Dumas, R. El Zein, H. Dallaporta, A. M. Charrier, *Langmuir* **2011**, *27*, 13643.

[13] A. Charrier, F. Thibaudau, *Biophys. J.* **2005**, *89*, 1094.

[14] R. El Zein, H. Dallaporta, A. M. Charrier, *J. Phys. Chem. B* **2012**, *116*, 7190.

[15] A. Charrier, T. Mischki, G. P. Lopinski, *Langmuir* **2010**, *26*, 2538.

[16] A. Kilic, M. F. Jadidi, H. O. Ozer, F. N. Kok, *Colloids. Surf. B.* **2017,** *160,* 117.

[17] M. T. L. Casford, A. Ge, P. J. N. Kett, S. Ye, P. B. Davies, *J. Phys. Chem. B* **2014**, *118*, 3335.

[18] M. Kiani, F. K. Harun, M. Ahmadi, M. Rahmani, M. Saeidmanesh, M. Zare, *Nanoscale Res. Lett.* **2014**, *9*, 371.

[19] E. Akbari, Z. Buntat, E. Shahraki, R. Parvaz, M. J. Kiani, *J. Biomater. Appl.* **2016**, *30*, 677.

[20] S. R. Tabaei, W. B. Ng, S.-J. Cho, N.-J. Cho, *ACS Appl. Mater. Interfaces* **2016**, *8*, 11875.

[21] Y. Zhang, S. Inal, C.-Y. Hsia, M. Ferro, M. Ferro, S. Daniel, R. M. Owens, *Adv. Funct. Mater.* **2016**, *26*, 7304.

[22] C. Kataoka-Hamai, Y. Miyahara, *Sci. Technol. Adv. Mater.* **2010**, *11*, 33001.

[23] S. Cotrone, M. Ambrico, H. Toss, M. D. Angione, M. Magliulo, A. Mallardi, M. Berggren, G. Palazzo, G. Horowitz, T. Ligonzo, L. Torsi, *Org. Electron.* **2012**, *13*, 638.

[24] M. Magliulo, K. Manoli, E. Macchia, G. Palazzo, L. Torsi, *Adv. Mater.* **2015**, *27*, 7528.

[25] M. Magliulo, A. Mallardi, M. Y. Mulla, S. Cotrone, B. R. Pistillo, P. Favia, I. Vikholm-Lundin, G. Palazzo, L. Torsi, *Adv. Mater.* **2013**, *25*, 2090.

[26] R. A. Böckmann, B. L. de Groot, S. Kakorin, E. Neumann, H. Grubmüller, *Biophys. J.* **2008**, *95*, 1837.

[27] S. J. Marrink, A. H. de Vries, D. P. Tieleman, *Biochim. Biophys. Acta*. **2009**, *1788*, 149.

[28] D. Needham, R. M. Hochmuth, *Biophys. J.* **1989**, *55*, 1001.

[29] R. W. Glaser, S. L. Leikin, L. V Chernomordik, V. F. Pastushenko, A. I. Sokirko, *Biochim. Biophys. Acta* **1988**, *940*, 275.

[30] J. Akinlaja, F. Sachs, *Biophys. J.* **1998**, *75*, 247.

[31] S. A. Akimov, P. E. Volynsky, T. R. Galimzyanov, P. I. Kuzmin, K. V. Pavlov, O. V. Batishchev, *Sci. Report*. **2017**, *7*, 12509.

[32] H. Kyun Kim, K. Kim, Y. Byun, *Biomaterials* **2005**, *26*, 3435.

[33] P. J. Clapp, B. A. Armitage, D. F. O'Brien, *Macromolecules* **1997**, *30*, 32.

[34] T. Nguyen Duc, R. El Zein, J.-M. Raimundo, H. Dallaporta, A. M. Charrier, *J. Mater. Chem. B* **2013**, *1*, 443.

[35] T. D. Nguyen, A. Labed, R. El Zein, S. Lavandier, F. Bedu, I. Ozerov, H. Dallaporta, J.-M. Raimundo, A. M. Charrier, *Biosens. Bioelectron.* **2014**, *54*, 571.

[36] A. Kenaan, T. D. Nguyen, H. Dallaporta, J.-M. Raimundo, A. M. Charrier, *Anal. Chem.* **2016**, *88*, 3804.

[37] S. Garcia-Manyes, F. Sanz, *Biochim. Biophys. Acta - Biomembr.* **2010**, *1798*, 741.

[38] H.-J. Butt, V. Franz, *Phys. Rev. E* **2002**, *66*, 31601.

[39] R. El Zein, Doctorate thesis: *Solid supported lipid monolayer: From biophysical properties to sensor application*, Aix Marseille University **2013**

[40] L. Venkataraman, J. E. Klare, I. W. Tam, C. Nuckolls, M. S. Hybertsen, M. L. Steigerwald, *Nano Lett.* **2006**, *6*, 458.

[41] H. B. Akkerman, A. J. Kronemeijer, P. A. van Hal, D. M. de Leeuw, P. W. M. Blom, B. de Boer, *Small* **2008**, *4*, 100.

[42] J. Chen, D. Yang, X. Ma, H. Li, D. Que, *J. Appl. Phys.* **2007**, *101*, 33526.

[43] M. Xiao, C. Qiu, Z. Zhang, L.-M. Peng, *ACS Appl. Mater. Interfaces* **2017**, *9*, 34050.

[44] D.K. Aswal, S. Lenfant, D. Guerin, J.V. Yakhmi, D. Vuillaume, *Anal. Chim. Acta* **2006**, 568, 84

[45] C. Boulas, J.V. Davidovits, F. Rondelez, D. Vuillaume, *Phys. Rev. Lett.* **1996**, 76, 4797

[46] M. Pavlin, T. Kotnik, D. Miklavčič, P. Kramar, A. Maček Lebar, ed. San Diego, CA: Elsevier; *Advances in Planar Lipid Bilayers and Liposomes* **2008**, 165.

[47] P. T. Vernier, M. J. Ziegler, Y. Sun, W. V. Chang, M. A. Gundersen, D. P. Tieleman, *J. Am. Chem. Soc.* **2006**, *128*, 6288.

[48] V. A. ZakrevskiĬ, N. T. Sudar, *Phys. Solid State* **2005**, 47, 961

[49] J. H. Klootwijk, J. F. Verweij, J. B. Rem, S. Bijlsma, *Microelectronics J.* **1996**, *27*, 623.

[50] J. Yota, H. Shen, R. Ramanathan, *J. Vac. Sci. Technol. A Vacuum, Surfaces, Film.* **2013**, *31*, 01A134.

[51] J. McPherson, J.-Y. Kim, A. Shanware, H. Mogul, *Appl. Phys. Lett.* **2003**, *82*, 2121.

[52] W. Huang, D. G. Levitt, *Biophys. J.* **1977**, *17*, 111.

[53] G. Gramse, A. Dols-Perez, M. A. Edwards, L. Fumagalli, G. Gomila, *Biophys. J.* **2013**, *104*, 1257.

[54] D. P. Tieleman, H. Leontiadou, A. E. Mark, S.-J. Marrink, *J. Am. Chem. Soc.* **2003**, *125*, 6382.

[55] S. Loi, G. Sun, V. Franz, H.-J. Butt, *Phys. Rev. E* **2002**, *66*, 31602.

[56] V. Franz, S. Loi, H. Müller, E. Bamberg, H.-J. Butt, *Colloids Surfaces B Biointerfaces* **2002**, *23*, 191.

[57] W. F. D. Bennett, N. Sapay, D. P. Tieleman, *Biophys. J.* **2014**, *106*, 210.

[58] N. Awasthi, J. S. Hub, *J. Chem. Theory Comput.* **2016**, *12*, 3261.

[59] H. J. Butt, M. Jaschke, Nanotechnology. **1995**, *6*, 1.

Table 1: Different types of lipid monolayers that were fabricated on top of H-terminated silicon. They differentiate by their head-groups and the number of reticulations. Their aliphatic chains (AC) represented by a black box are all identical and contain acetylenic groups. Each layer thickness was determined by making a hole in the layer using an AFM tip.

	DC-PC	**DC-Glycerol**	**DC-Glycerol-R**	**DC-MTS**	**DC-OTS**
Lipid layers	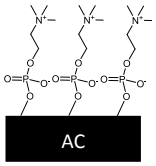	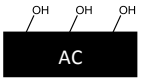	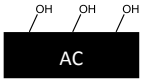	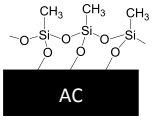	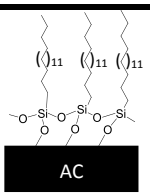
Reticulation **1**	-	-	✓	✓	✓
Reticulation **2**	-	-	-	✓	✓
Layer thickness [nm]	2.6±0.2	2.2±0.2	2. 2±0.2	2.2±0.2	4.3±0.3

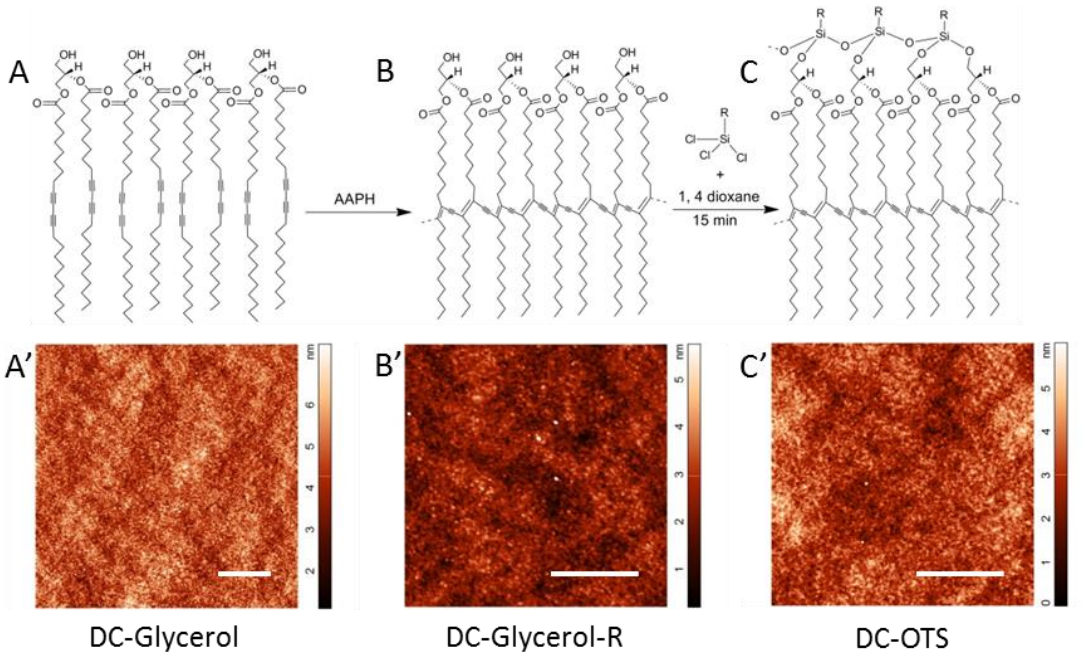

Figure 1 (A-C) Scheme representing the two-stage reticulation process of a lipid monolayer with (A'-C') the corresponding AFM images. First, acetylenic groups of DC-glycerol lipid aliphatic chains are reticulated (Reticulation 1) using free radical AAPH for activation. Second, trichlorosilane derivative such as MTS or OTS is use to functionalize hydroxyl functions at lipid head-groups leading to second reticulation. A' was measured in solution using a liquid cell, B' and C' in air. The surface roughness is 0.69, 0.48 and 0.61 nm for DC-glycerol, Dc-glycerol-R and DC-OTS respectively. Scale bar is 1 µm.

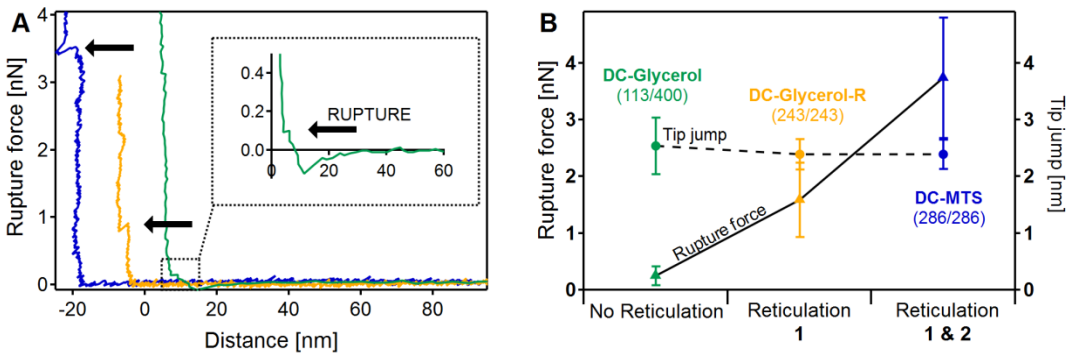

Figure 2 a) Examples of force versus indentation curves obtained on DC-Glycerol (Green), DC-Glycerol-R (Yellow) and DC-MTS (Blue). For clarity, the curves have been shifted along the x-axis. The layer rupture shows as a jump in the distance as indicated by black arrows. b) Average forces extracted from indentation measurements by AFM to rupture monolayers of non-reticulated (Green) and reticulated (Reticulation **1**) DC-Glycerol layers (Yellow) and DC-MTS layers (Reticulations **1** & **2**, Blue). Numbers are: N° of useful data/N° of measurements (For DC-Glycerol the rupture force was often smaller than the resolution of our experimental setup and hence non-measurable).

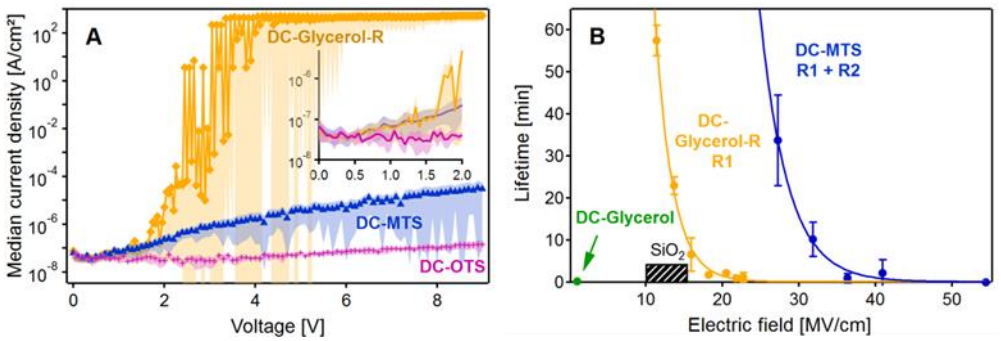

Figure 3 a) Leakage current density (Log scale) measured across DC-Glycerol-R, DC-MTS and DC-OTS lipid monolayers supported on silicon. Each curve represents the median curve and the error bars (colored areas), the median absolute deviation of at least 20 measurements. b) Lifetime of DC-Glycerol, DC-Glycerol-R and DC-MTS layers in a constant electric field. Each point corresponds to an average of at least 5 measurements.

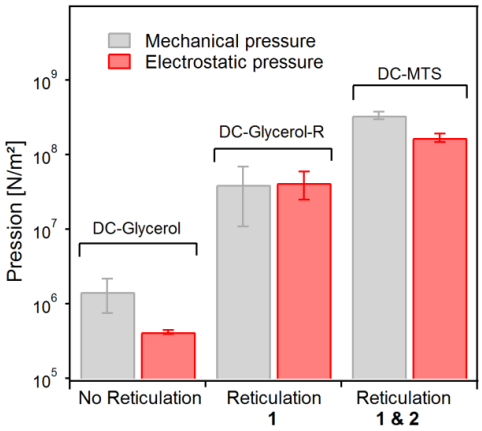

Figure 4 Mechanical and electrostatic pressures calculated for the rupture force and direct breakdown electric field respectively for the DC-Glycerol, DC-Glycerol-R and DC-MTS layers. Each result is the average of a minimum of 5 independent measurements.

Table of contents entry

The development of ultra-thin engineered lipid monolayers with exceptional mechanical and dielectric properties to be used as ultrathin dielectric is reported. The layers are obtained by a simple two-stage reticulation process. A relationship between mechanical and dielectric performances is demonstrated.

Keyword: Ultra-thin lipid based dielectric

A. Kenaan, R. El Zein, V. Kilinc, S. Lamant, J.-M. Raimundo*, A.M. Charrier*

Title: Ultra-thin supported lipid monolayer with unprecedented mechanical and dielectric properties